(14) Gervais, M.; Douy, R.; Gallot, B.; Erre, R. *Polymer* **1986**, *27*, 1513.
(15) Kugo, K.; Hata, Y.; Hayashi, T.; Nakajima, A. *Polym. J.* **1982**, *14*, 401.
(16) Gaines, G. L., Jr.; Bender, G. W. *Macromolecules* **1972**, *5*, 82.
(17) Yamashita, Y. *J. Macromol. Sci., Chem.* **1979**, *A13*, 401.
(18) Owens, D. K. *J. Appl. Polym. Sci.* **1970**, *14*, 185.
(19) Kendrick, T. C.; Kingston, B. M.; Lloyd, N. C.; Owen, M. J. *J. Colloid Interface Sci.* **1967**, *24*, 135.
(20) Gaines, G. L., Jr. *Macromolecules* **1981**, *14*, 1366.
(21) Fredrickson, G. H. *Macromolecules* **1987**, *20*, 2535.
(22) Gaines, G. L., Jr. *J. Phys. Chem.* **1969**, *73*, 3143.
(23) Gaines, G. L., Jr. *J. Polym. Sci. Part A-2* **1969**, *7*, 1379.
(24) Siow, K. S.; Patterson, D. *J. Phys. Chem.* **1973**, *74*, 356.
(25) Ober, R.; Paz, L.; Taupin, C.; Pincus, P.; Boileua, S. *Macromolecules* **1983**, *16*, 50.
(26) DiMeglio, J. M.; Ober, R.; Paz, L.; Taupin, C.; Pincus, P.; Boileau, S. *J. Phys.* (*Les Ulis, Fr.*) **1983**, *44*, 1035.
(27) Koberstein, J. T. In *Encyclopedia of Polymer Science and Engineering*; Wiley: New York, 1987; Vol. 8, p 237.
(28) Busscher, H. J.; Hoogsteen, W.; Dijkema, L.; Sawatsky, G. A.; van Pelt, A. W. J.; de Jong, H. P.; Challa, G.; Arends, J. *Polym. Commun.* **1985**, *26*, 252.
(29) LeGrand, D. G.; Gaines, G. L., Jr. *J. Polym. Sci., Part C* **1971**, *34*, 45.
(30) Flory, P. J. *Principles of Polymer Chemistry*; Cornell University Press: Ithaca, NY, 1953.
(31) Pan, D. H.; Prest, M. W., Jr. *J. Appl. Phys.* **1985**, *58*, 15.
(32) McMaster, L. P. *Macromolecules* **1973**, *6*, 760.
(33) Nishi, T.; Wang, T. T.; Kwei, T. K. *Macromolecules* **1975**, *8*, 227.
(34) Kwei, T. K.; Wang, T. T. In *Polymer Blends*; Paul, D. R., Newman, S., Eds.; Academic: New York, 1978; Vol. 1.
(35) Hadziioannou, G.; Stein, R. *Macromolecules* **1984**, *17*, 567.
(36) Shiomi, T.; Kohno, K.; Yoneda, K.; Tomita, T.; Miya, M.; Imai, K. *Macrmolecules* **1985**, *18*, 414.
(37) Jelenic, T.; Kirste, R. G.; Oberthuer, R. C.; Schmitt-Streeker, S.; Schmitt, B. J. *Makromol. Chem.* **1984**, *12*, 185.
(38) Bhatia, Q. S.; Chen, J. K.; Koberstein, J. T.; Sohn, J. E.; Emerson, J. A. *J. Colloid Interface Sci.* **1985**, *106*, 352.
(39) Anastasiadis, S. H.; Chen, J. K.; Koberstein, J. T.; Sohn, J. E.; Emerson, J. A. *Polym. Eng. Sci.* **1986**, *26*, 1410.
(40) Anastasiadis, S. H.; Chen, J. K.; Koberstein, J. T.; Sohn, J. E.; Emerson, J. A.; Siegel, A. F. *J. Colloid Interface Sci.* **1987**, *119*, 55.
(41) Bender, G. W.; Gaines, G. L., Jr. *Macromolecules* **1970**, *3*, 128.
(42) Van Krevelen, D. W. *Properties of Polymers*; Elsevier: Amsterdam, 1976.
(43) Kwei, T. K.; Nishi, T.; Roberts, R. F. *Macromolecules* **1974**, *7*, 667.
(44) Hartland, S.; Hartley, R. W. *Axisymmetric Fluid-Liquid Interface*; Elsevier: Amsterdam, 1976.
(45) Cahn, J. W. *J. Chem. Phys.* **1977**, *66*, 3667.
(46) Poser, C. I.; Sanchez, I. C. *Macromolecules* **1981**, *14*, 361.
(47) de Gennes, P.-G. *Macromolecules* **1981**, *14*, 1637.
(48) Bhatia, Q. S. Ph.D. Thesis, Princeton University, 1987.
(49) Clark, D. T.; Dilks, A. *J. Polym. Sci., Polym. Chem. Ed.* **1976**, *14*, 533.
(50) Wagner, C. D.; Riggs, W. M.; Davis, L. E.; Moulder, J. F.; Muilenberg, J. E. *Handbook of X-ray Photoelectron Spectroscopy*, Perkin-Elmer Corp., 1979.
(51) Proctor, A.; Sherwood, P. M. A. *Anal. Chem.* **1982**, *54*, 13.
(52) Clark, D. T.; Thomas, H. R.; Dilks, A.; Shuttleworth, D. J. *Electron Spectrosc. Relat. Phenom.* **1971**, *10*, 435.
(53) LeGrand, D. G.; Gaines, G. L., Jr. *J. Colloid Interface Sci.* **1969**, *31*, 162.
(54) Wu, S. In *Polymer Blends*; Paul, D. R., Newman, S., Eds., Academic: New York, 1978.
(55) Goldblatt, R. D.; Scilla, G. J.; Park, J. M.; Johnson, J. N.; Huang, S. *J. Appl. Polym. Sci.*, in press.
(56) Fadley, C. S.; Bergström, S. A. L. *Phys. Lett. A* **1971**, *35a*, 375.
(57) Fadley, C. S. *Prog. Surf. Sci.* **1984**, *16*, 275.
(58) Clark, D. T.; Thomas, H. R. *J. Polym. Sci., Polym. Chem. Ed.* **1977**, *15*, 2843.
(59) Szajman, J.; Liesegang, J.; Jenkin, J. G.; Leckey, R. G. G. *J. Electron Spectrosc. Relat. Phenom.* **1978**, *14*, 247.
(60) Fadley, C. S.; Baird, R. J.; Sickhaus, W.; Novakov, T.; Bergström, S. A. L. *J. Electron Spectrosc.* **1974**, *4*, 93.
(61) Edwards, S. F. *Proc. Phys. Soc., London* **1966**, *88*, 265.
(62) Edwards, S. F.; Jeffers, E. F. *J. Chem. Soc., Faraday Trans. 2* **1979**, *75*, 1020.
(63) Daoud, M.; Jannink, G. *J. Phys.* (*Les. Ulis, Fr.*) **1975**, *37*, 973.
(64) Schaefer, D. W. *Polymer* **1984**, *25*, 387.
(65) Hashimoto et al., unpublished results quoted by Schichtel; Binder, *Macromolecules* **1987**, *20*, 1679.
(66) Schwan, D., et al. *J. Chem. Phys.*, in press.

Entanglement in Blends of Monodisperse Star and Linear Polystyrenes. 1. Dilute Blends

Hiroshi Watanabe,[†] Hirotsugu Yoshida, and Tadao Kotaka*

Department of Macromolecular Science, Faculty of Science, Osaka University, Toyonaka, Osaka 560, Japan.

Received October 1, 1987; Revised Manuscript Received January 19, 1988

ABSTRACT: Viscoelastic properties of binary blends composed of narrow molecular weight distribution (MWD) 4-arm star polystyrenes (2-chain) of molecular weight (MW) M_2 and narrow MWD linear polystyrenes (1-chain) of M_1 were examined and compared with binary blends of narrow MWD linear polystyrenes of M_2 and M_1. In these blends, the volume fraction ϕ_2 of the 2-chain was kept small so that the 2-chains were entangling only with the matrix 1-chains but not with themselves. When the MW of the components of these dilute blends were such that $M_c < M_1 \ll M_2$, with M_c being the characteristic MW, the star 2-chain exhibited Rouse–Ham-like relaxation modes with the (weight average) relaxation time proportional to $\phi_2{}^0 M_1{}^3 M_2{}^2$ and the compliance proportional to $\phi_2{}^{-1} M_1{}^0 M_2$. Similar behavior was also found in the dilute blends of linear chains. These results suggest that the star as well as the high-MW linear (2-) chain in the dilute blend with $M_2 \gg M_1 > M_c$ may relax as the surrounding 1-chains diffuse away so that the 1–2 entanglement has become ineffective. In the framework of the generalized tube model, this relaxation mechanism corresponds to the *tube renewal* mode. The limiting ratio of M_2/M_1, for which these power laws are valid, is smaller for the star/linear chain blends than that for the linear chain blends. This is because the intrinsic relaxation time of the star 2-chain of M_2 is longer than that of the linear 2-chain of the same M_2, observed in the bulk states. Thus, the star 2-chain exhibits the Rouse–Ham modes more easily than the corresponding linear 2-chain in the same matrix 1-chains.

Introduction

Blends of narrow molecular weight distribution (MWD) polymers are simple but important model systems for examining the effects of *entanglement* on the relaxation behavior of condensed polymer systems.[1-11] Recently, several groups including ourselves studied viscoelastic[3-11] and diffusion[12-15] properties of binary blends of narrow MWD linear polymers of high and low MW. In such a blend the terminal relaxation modes of the high-MW chain (the test chain) are strongly affected by the lifetime of the

---

[†] On leave from the Department of Chemical Engineering and Materials Science, 151 Amundson Hall, University of Minnesota—Twin Cities, 421 Washington Ave. S.E., Minneapolis, MN 55455.

0024-9297/88/2221-2175$01.50/0

entanglement network formed in the blends.

Another important factor governing the relaxation modes in condensed polymer systems is the *topological* type of the test chain itself, such as linear, branched, star,[16-20] H shaped,[21] and ring.[22,23] Especially, bulk star-polymer systems were examined extensively, and the following features were revealed.[16-20] The compliance is proportional to the arm molecular weight M_a of the star molecules and described by the Rouse–Ham theory,[24,25] while the relaxation times and viscosity increase exponentially with M_a,[18] differing from linear-chain polymer systems for which the relaxation times and viscosity often obey power laws with respect to the molecular weight.[1]

To examine the effects of these two factors on the terminal relaxation modes of condensed polymer systems, we extended our studies on binary[3-6] and ternary[7] blends of linear narrow MWD polystyrenes (PS) to those of star and linear polystyrenes.

In this study, we have examined the behavior of binary blends consisting of high-MW 4-arm star PS chains diluted in low-MW linear PS matrices. The volume fraction of the star chain, ϕ_2, was always kept small so that the star chains entangled only with the matrix chains but not with themselves. We have two purposes in mind: One was to examine the features of the relaxation mechanisms in such blends due to disentanglement of the test chain from the entanglement network formed by the matrix chains; the other was to compare the features of the intrinsic relaxation modes of the star versus linear chains in such dilute blends.

In terms of the generalized tube theory,[26] the former process was often called *constraint release by tube renewal*.[26-28] On the other hand, for the latter problem, Ham developed a theory for the intrinsic relaxation modes of an isolated star chain,[25] but the theory has not yet been critically tested for star/linear chain blends. Thus in this article we will compare the relaxation behavior of the star versus high-MW linear PS chains in the matrices of low-MW linear PS chains.

Experimental Section

Materials. Anionic polymerization was carried out in preparing narrow MWD 4-arm star PS samples.[29,30] Styrene monomer, benzene, methanol, and other chemicals for the anionic polymerization were purified by the methods recommended by Fetters[31] and by Fujimoto[32] as described in our previous papers.[33] 1,2-Bis(trichlorosylyl)ethane (bTSE) was used as the coupling agent for polystyryl anions. The reagent was purified by repeating sublimation under high vacuum twice, dissolved in purified hexane, and stored in an ampule. The concentration of bTSE was determined by titration with aqueous solution of sodium hydroxide.

Star PS samples were prepared via the following procedures. First, anionic polymerization of styrene was carried out in benzene by using *sec*-butyllithium as the initiator. After 48 h of reaction at ambient temperature, an aliquot was taken from the mixture to recover the precursor PS sample for the convenience of later characterization. A prescribed amount of bTSE in hexane was then added and allowed to react with the rest of the polystyryl anions.

Gervasi and Gosnell[29] reported that in the coupling reaction of polystyryl anions with bTSE, the maximum number of arms attained was only 4, in spite of the fact that the coupling agent used was hexafunctional. This is because the reaction rate of especially the last two chlorines with polystyryl anions became extremely slow as the coupling reaction proceeded. On the other hand, in the coupling of polyisoprenyl anions with bTSE to obtain star polyisoprene (PI) samples, 6-arm star samples were easily obtained.[30] This difference in the coupling behavior may be due to the difference in the steric hindrance of very long PS versus PI chains. In our experiments, this fact was successfully utilized for checking the purity of bTSE.

Table I
Characteristics of 4-Arm Star Polystyrene Samples

code[a]	$10^{-3}M_w$	M_w/M_n	f[b]	$[\eta]$[c]
4S77	307	1.08	4.2	
4S184	736	1.05	4.0	1.52
4S310	1240	1.06	4.1	2.08
4S410	1640	1.07	4.2	2.51
4S662	2650	1.06	3.9	3.92

[a] The code number indicates the rounded number of the arm molecular weight $M_a = M_w/4$ in units of 1000. [b] $f = (M_w)_{star}/(M_w)_{precursor}$. [c] Intrinsic viscosity (in 100 cm^3/g) in toluene 35 °C.

Coupling of polystyryl anions with the hexafunctional bTSE yielded, at most, 4-arm star PS samples. Thus, to avoid contamination with components with less arms, we adjusted the mole ratio of the chlorine atoms of bTSE to the polystyryl anions so that there was a large excess of the latter over the former, typically from $^1/_2$ to $^1/_5$. We kept the mixture at 35 °C under gentle stirring for 2 weeks to 2 months, depending on MW of the precursor PS.

Each crude reaction product prepared under such a condition inevitably contained a large amount of precursor PS and other undesired components. Thus, the crude product was subjected to fractionation by using benzene (BZ) and methanol (MeOH) to separate the desired 4-arm star component in as pure form as possible. In a typical run, starting with approximately 5 g/L of BZ solution of the crude product, we added MeOH to make the BZ:MeOH volume ratio approximately 4:1, equilibrated at the ambient temperature, and recovered the gel phase. This procedure was repeated three times, during which nearly all the precursor was removed. Finally to remove possible high-MW contaminant, we recovered the dilute solution phase from the phase-separated mixture.

Characterization of the Samples. The polymer samples were characterized by using a gel permeation chromatograph (GPC, Tosoh Co., Model HLC-801A) equipped with a triple-detector system consisting of a UV monitor (Tosoh Co., Model UV-8) and a low-angle laser-light-scattering (LALLS) photometer (Tosoh Co., Model LS-8000) with a built-in refractometer. The elution solvent was chloroform, and commercially available standard PS samples (Tosoh Co., TSK PS) were used as the elution standards. The weight average molecular weight, M_w, and the M_w at each elution volume were determined by using the LALLS monitor. The results of the GPC characterization of the star PS samples are summarized in Table I.

Intrinsic viscosities, $[\eta]$, of the purified star PS fractions were determined in toluene at 35 °C. The results are also listed in Table I. The $[\eta]$ versus M_w data for the star PS samples are in good agreement with those reported by Roovers and Bywater.[34]

To evaluate the heterogeneity of the samples, we also carried out sedimentation velocity experiments at 35.0 °C in cyclohexane on a Beckman–Spinco Model E analytical ultracentrifuge.[33] The polymer concentration were 0.0629 to 0.144 × 10^{-2} g cm^{-3}.

As an example, Figure 1 (left) shows gel permeation chromatograms of a crude reaction product and its star PS fraction prepared from a precursor PS sample of $M_w = 389 \times 10^3$. The circles in the figure indicate the M_w of the fractions at each elution count. Figure 1 (right) shows sedimentation velocity patterns of the same samples. As seen in this figure, the crude product might be contaminated with 3-arm star and/or dimer components besides the precursor. However, the chromatogram and sedimentation pattern of the purified star fraction suggest that the contaminants have been thoroughly removed during the fractionation procedure. The $(M_w)_{star}/(M_w)_{precursor}$ ratios, f, in Table I suggest that the 4-arm star samples are reasonably pure.

Beside these star PS samples, we also used some narrow-MWD linear PS samples, some of which were prepared by ourselves,[33] and some of which were commercially available samples. The molecular characteristics of these linear PS samples are summarized in Table II. The MWD of all the samples used are sufficiently narrow, as judged from the ratios of the weight average to number average molecular weight, M_w/M_n, shown in these tables. Thus, in the followings, we designate all the 4-arm star (4S) and linear (L) narrow MWD PS samples as *monodisperse* and will not distinguish M_w and M_n. The linear PS samples are coded, for example, as L2810 with the number representing M_w,

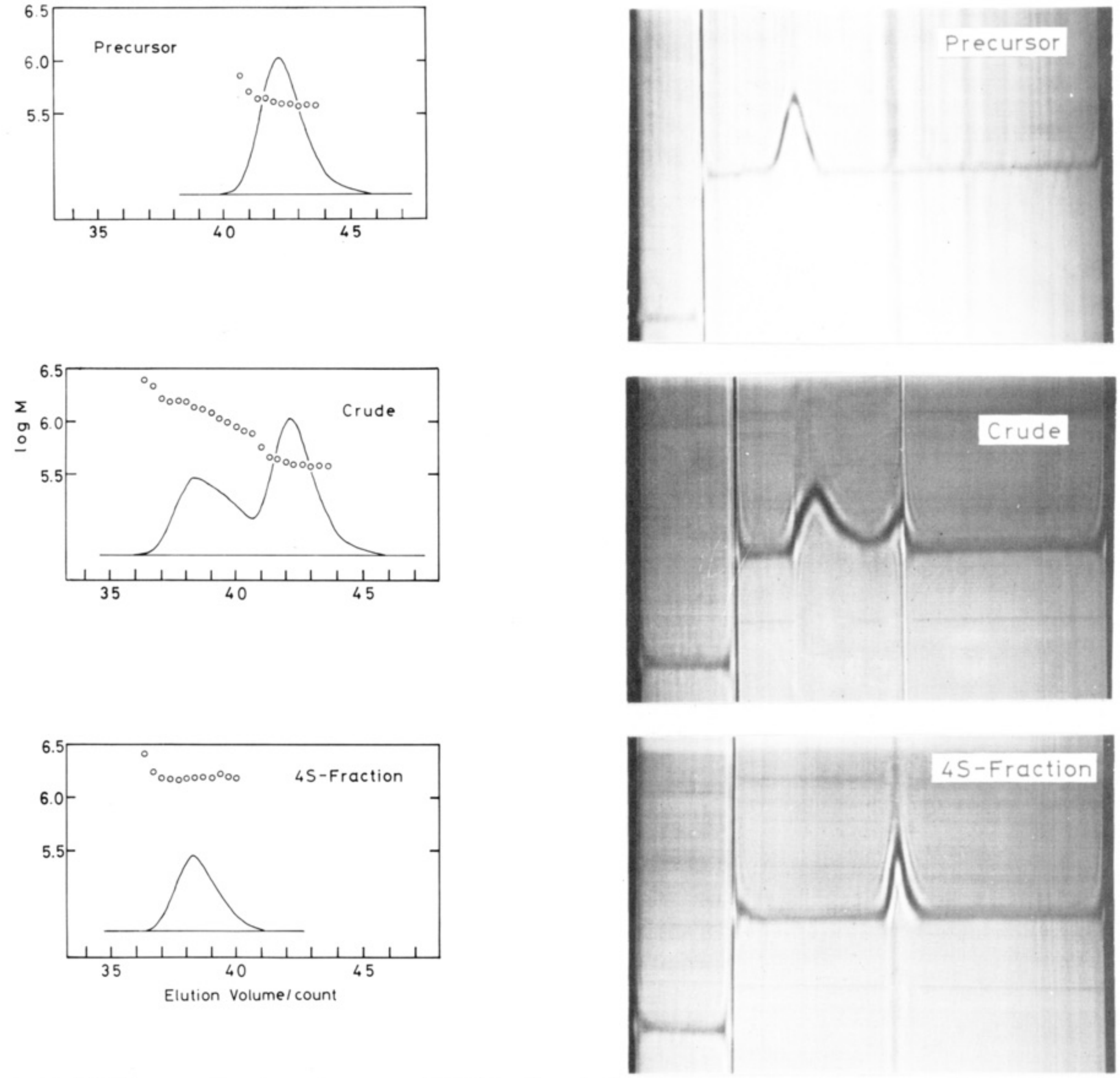

Figure 1. (Left) Gel permeation chromatograms and (right) sedimentation velocity patterns of the precursor L389 of the 4S410 star sample (top), the crude reaction product (center), and the purified 4S410 star fraction (bottom). The circles in the left half indicate M_w of the fraction at each elution count.

Table II
Characteristics of Linear-Chain Polystyrene Samples

code[a]	$10^{-3}M_w$	M_w/M_n	code[a]	$10^{-3}M_w$	M_w/M_n
L5[b]	5.2	1.08	L89[b]	88.5	1.07
L11[b]	10.5	1.08	L110[c]	110	1.06
L23	23.4	1.07	L124[b]	124	1.05
L26	26.3	1.06	L172[b]	172	1.07
L42	41.5	1.06	L315[b]	315	1.07
L46[b]	46.0	1.05	L775[b]	775	1.01
L72	72.4	1.06	L2810[b]	2810	1.09

[a] The code number indicates the rounded number of the weight average molecular weight M_w in units of 1000. [b] From Tosoh Co. [c] From Pressure Chemicals Co.

and the 4-arm star samples as 4S410 with the arm molecular weight, $M_a = M_w/4$, both with the unit 1000. Thus, M_a does not necessarily agree with $(M_w)_{\text{precursor}}$.

Rheological Measurements. Dynamic measurements were carried out on a laboratory rheometer (Model IR-200: Iwamoto Seisakusho, Ltd., Kyoto) of a cone and plate type, similar to the one described previously.[3-6]

The systems examined were blends composed of the fractionated 4-arm star (4S) samples or high-MW linear PS (L) samples as the test (2-) chain and the low-MW linear PS (L) samples as the matrix (1-) component. As the reference, the pure 4S and L samples were also examined.

First, we attempted to carry out the measurement on molten bulk systems. However, the high-MW 4S samples did not relax in the temperature and frequency ranges accessible to the present experiment. In fact, the high-MW samples often degraded within 2 h at the temperatures above 200 °C. Thus, we added to the systems dibutyl phthalate (DBP) as a plasticizer.[6,7] For a few blends of much higher MW, we used dioctyl phthalate (DOP) as a less volatile plasticizer. The measurements were carried out in the temperature ranges between 15 and 90 °C for the DBP systems and between 35 and 150 °C for the DOP systems.

The weight fraction of the plasticizer was always 40 wt % for the DBP systems and 38.5 wt % for the DOP systems, so that the volume fraction ϕ_p of the polymer component (1 + 2 chains) was always 60 vol %. Here, we neglected the volume change upon mixing the components. The characteristic molecular weight M_c and the entanglement spacing M_e for these plasticized blends were 51×10^3 and 30×10^3, respectively, for the DBP and DOP systems.[1]

The time–temperature superposition principle[1] was applied to obtain master curves of the storage G' and loss G'' moduli. All the data were reduced to an isofriction state with the free-volume fraction $f_r = 0.0644$. Although the results are not shown here, the shift factor a_T was well represented by the previously reported

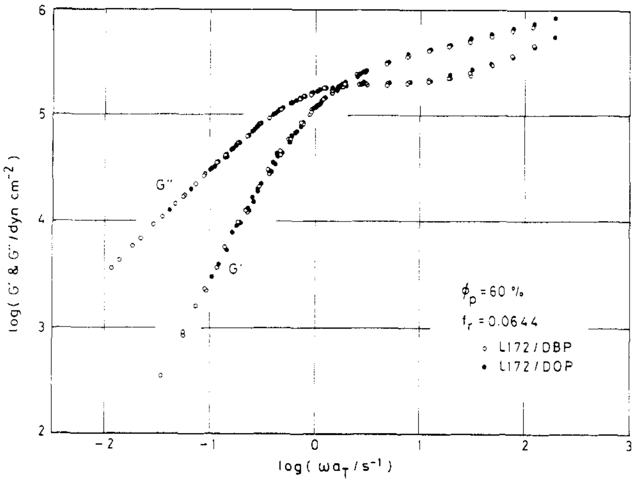

Figure 2. Comparison of the G' and G'' master curves of L172/DBP and L172/DOP systems with ϕ_p = 60 vol % to see the effect of the difference in the plasticizer.

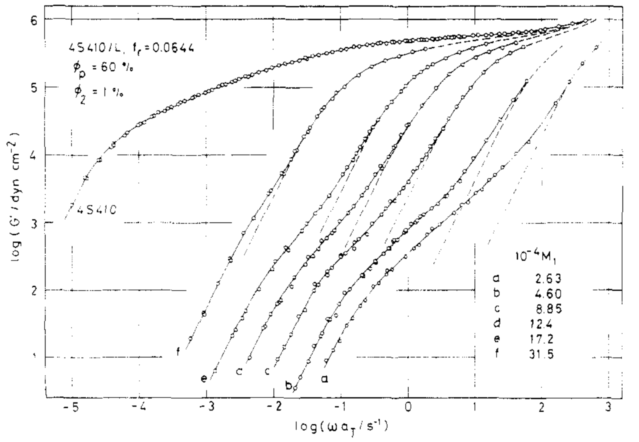

Figure 3. Master curves of the storage moduli G' for 4S410/L blends with ϕ_p = 60 vol % and ϕ_2 = 1 vol % at the reference temperature T_r.

WLF equation: $\log a_T = -6.74(T - T_r)/(133.6 + T - T_r)$.[5,6] The reference temperatures T_r were 54 and 71 °C, respectively, for the DBP and DOP plasticized systems with $M_1 > 23.4 \times 10^3$ and ϕ_p = 60 vol %.

Figure 2 compares the G' and G'' master curves for L172/DBP and L172/DOP systems with ϕ_p = 60 vol % at their respective T_r. We notice that the viscoelastic behavior at the T_r are the same for the two systems. Thus, in the following, we do not distinguish the difference in the plasticizer when the data were reduced to the T_r.

Results

Complex Moduli of the Dilute Blends. Figure 3 shows the master curves of dynamic moduli, $G'(\omega a_T)$, in a double logarithmic scale for the blends of 4S410 and different L samples with ϕ_2 = 1 vol % and for the pure 4S410 sample, all with ϕ_p = 60 vol %. The broken curves indicate those for the pure 1-chains ($\phi_p = \phi_1$ = 60 vol %) as the reference. Such systems will be referred to as the parent-monodisperse (p-m) systems for the blends.

Comparing each blend with its p-m system, we see that the behaviors at high frequencies coincide with each other, but slow relaxation modes due to the 2-chain prevail as a shoulder at the low-frequency end of the G' curve. Although not shown here, similar but less-enhanced trends were observed in the G'' master curves of the blends and their p-m systems.

The agreement found between the G' curves of the blends and p-m systems in the high-frequency region suggests that the relaxation modes of the 1-chain in the blends with $\phi_1 \gg \phi_2$ are nearly the same as those in the p-m systems. Thus, for these dilute blends we may use the previously proposed blending law[5,6]

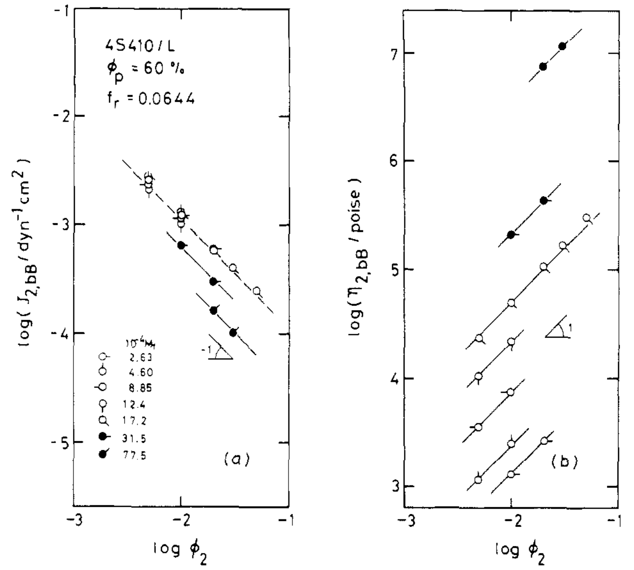

Figure 4. Dependences on ϕ_2 of (a) the compliance $J_{2,bB}$ and (b) the viscosity $\eta_{2,bB}$ of the star 2-chain in 4S410/L blends (with ϕ_p = 60 vol % but varying ϕ_2) at the reference temperature T_r.

$$H_{bB}(\tau) = \phi_1 H_{1,m}(\tau) + \phi_2 H_{2,bB}(\tau) \tag{1}$$

Here, H_{bB} is the relaxation spectrum of the blend, $H_{1,m}$ the spectrum of the 1-chain in the p-m system, and $H_{2,bB}$ the spectrum of the 2-chain in the blend. Note that $H_{1,m}$ and $H_{2,bB}$ are the spectra reduced to the *unit volume* of the 1- and 2-chains, respectively. Thus, for example, the storage modulus, $G'_{1,m}$, of the p-m system with the content of the 1-chain $\phi_1 = \phi_p$ can be given by

$$G'_{1,m}(\omega) = \phi_p \int_{-\infty}^{\infty} H_{1,m}(\tau) \frac{\omega^2\tau^2}{1 + \omega^2\tau^2} \, d \ln \tau \tag{2}$$

By using eq 1, we can define the contribution of the 2-chain to the dynamic moduli, $G'_{2,bB}$, and loss moduli, $G''_{2,bB}$, as follows:

$$G'_{2,bB}(\omega) = \phi_2 \int_{-\infty}^{\infty} H_{2,bB}(\tau) \frac{\omega^2\tau^2}{1 + \omega^2\tau^2} \, d \ln \tau = G'_{bB}(\omega) - (\phi_1 G'_{1,m}/\phi_p) \tag{3a}$$

$$G''_{2,bB}(\omega) = \phi_2 = \int_{-\infty}^{\infty} H_{2,bB}(\tau) \frac{\omega\tau}{1 + \omega^2\tau^2} \, d \ln \tau = G''_{bB}(\omega) - (\phi_1 G''_{1,m}/\phi_p) \tag{3b}$$

Here, G'_{bB} and G''_{bB} are the observed moduli for the blend, and $G'_{1,m}$ and $G''_{1,m}$ are those for the corresponding p-m system.

Then, from eq 1–3, we can define the contributions of the 2-chain in the blend to the viscosity, $\eta_{2,bB}$, the elastic coefficient, $A_{2,bB}$, and the compliance, $J_{2,bB}$, as follows:[6]

$$\eta_{2,bB} = \eta_{bB} - (\phi_1 \eta_{1,m}/\phi_p) \tag{4a}$$

$$A_{2,bB} = A_{bB} - (\phi_1 A_{1,m}/\phi_p) \tag{4b}$$

$$J_{2,bB} = A_{2,bB}/(\eta_{2,bB})^2 \tag{4c}$$

Thus, the quantities $\eta_{2,bB}$, $A_{2,bB}$, and $J_{2,bB}$ can be calculated directly from the corresponding quantities of the bB and p-m systems (which are evaluated from the observed G' and G'' curves in the low-frequency ends) without actually

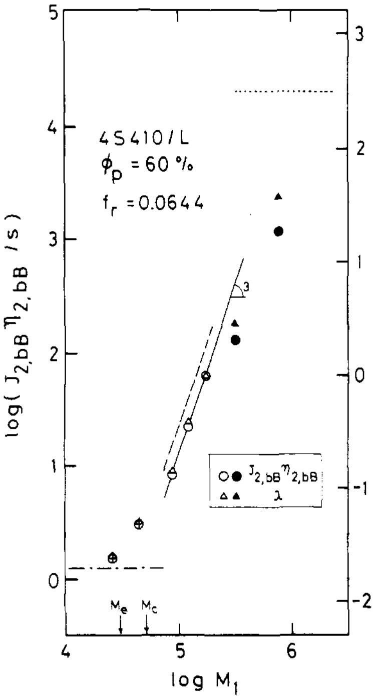

Figure 5. M_1 dependence of the weight average relaxation time $J_{2,bB}\eta_{2,bB}$ of the 2-chain in dilute 4S410/L blends (represented by circles). The horizontal dotted line indicates the relaxation time of the monodisperse 4S410 system with $\phi_p = 60$ vol %; the triangles indicate the shift factor λ to superpose the low-frequency ends of the $\phi_2^{-1}G'_{2,bB}$ curves (see Figure 8 and the text). The broken line indicates the relaxation times of the Rouse–Ham modes estimated for the 4S410 chain by applying eq 9 to the data of the dilute L2810/L blends of $M_c < M_1 \ll M_2$, in which 1- and 2-chains are well entangled; the dash-dot line indicates the relaxation time estimated from the dilute L2810/L blends with $M_1 < M_e$, in which there is no entanglement between the 1- and 2-chains.

calculating the relaxation spectra, H_{bB} and $H_{1,m}$.

Figure 4 shows plots of (a) $J_{2,bB}$ and (b) $\eta_{2,bB}$ versus the 2-chain content ϕ_2 for 4S410/L blends evaluated by eq 4. We notice that $J_{2,bB}$ and $\eta_{2,bB}$ are roughly proportional to ϕ_2^{-1} and ϕ_2, respectively, in the range $\phi_2 < 5$ vol %. However, after ϕ_2 has exceeded 5 vol %, $\eta_{2,bB}$ appears to increase more rapidly with ϕ_2. This result suggests that in the blends with $\phi_2 < 5$ vol % no entanglement between the 2-chains is existing so that $H_{2,bB}$ does not change with ϕ_2.[35] Hence, hereafter we refer to such a blend as the *dilute* blend.

Weight Average Relaxation Times. From eq 4a–c, we can define the (weight average) relaxation time, $J_{2,bB}\eta_{2,bB}$, of the 2-chain in the blend as

$$J_{2,bB}\eta_{2,bB} = A_{2,bB}/\eta_{2,bB} = \int_{-\infty}^{\infty} H_{2,bB}\tau^2 \, d \ln \tau \Big/ \int_{-\infty}^{\infty} H_{2,bB}\tau \, d \ln \tau \quad (4d)$$

Figures 5 and 6, respectively, show the M_1 and M_2 dependences of $J_{2,bB}\eta_{2,bB}$ of the 4S component (2-chain) in dilute 4S/L blends (indicated by the circles). The weight average relaxation times were independent of ϕ_2 for the dilute blends with $\phi_2 < 5.0$ vol %. In Figure 7, the M_1 dependence of $J_{2,bB}\eta_{2,bB}$ of the linear 2-chain in dilute L2810/L blends (with $\phi_2 = 1.0$ vol % and $\phi_p = 60$ vol %) is shown for the sake of comparison.

For convenience, all the numerical data on the viscoelastic constants of the 4S/L blends systems and of the L/L blends[6] are summarized in Tables III and IV, respectively, including the data on the shift factor, log λ, discussed later in relation with Figures 8 and 9. In Table V, we summarize the zero-shear viscosity η_m and steady-state compliance J_m of the monodisperse 4S410 and other L samples with $\phi_p = 60$ vol %.

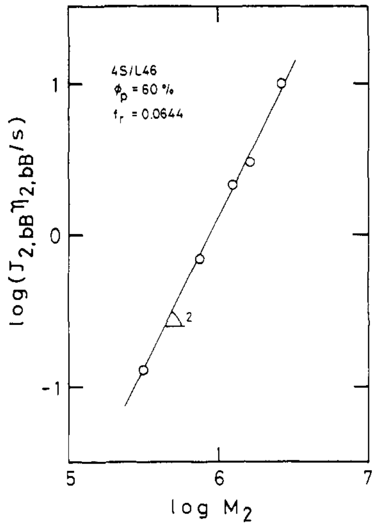

Figure 6. M_2 dependence of the weight average relaxation time $J_{2,bB}\eta_{2,bB}$ of the 2-chain in dilute 4S/L46 blends.

Table III
Zero-Shear Viscosity η_{bB}/P, Steady-State Compliance J_{bB}/(dyn^{-1} cm^2) of 4S/L Blends, and Compliance $J_{2,bB}$, Weight Average Relaxation Time $J_{2,bB}\eta_{2,bB}$/s, and Shift Factor λ of 4S Chain in the 4S/L Blends with ϕ_P = 60 vol % at T_r of an Isofree Volume Fraction State of f_r = 0.0644

matrix[a]	ϕ_2	log η_{bB}	log J_{bB}	log $J_{2,bB}$	log ($J_{2,bB}\eta_{2,bB}$)	log λ
			4S77/L Blends			
L46	5	4.11	−5.24	−4.74	−0.89	
			4S184/L Blends			
L46	0.5	3.85	−4.90	−3.07	−0.15	
	1.0	3.90	−4.70	−3.40	−0.16	
			4S310/L Blends			
L46	1.0	3.93	−4.17	−3.03	0.33	
			4S410/L Blends			
L26	1.0	3.53	−3.76	−2.92	0.19	−1.62
	2.0	3.67	−3.72	−3.22	0.20	
L46	0.5	3.87	−4.20	−2.59	0.47	
	1.0	3.94	−3.99	−2.91	0.49	−1.33
L89	0.5	4.57	−4.64	−2.64	0.91	
	1.0	4.61	−4.40	−2.94	0.93	−0.88
L124	0.5	5.04	−4.66	−2.68	1.34	
	1.0	5.08	−4.45	−3.00	1.34	−0.44
L172	0.5	5.53	−4.75	−2.56	1.84	
	1.0	5.56	−4.53	−2.89	1.83	
	2.0	5.62	−4.36	−3.24	1.81	0
	3.0	5.68	−4.25	−3.40	1.85	
	5.0	5.79	−4.17	−3.61	1.90	
L315	1.0	6.42	−5.08	−3.17	2.17	
	2.0	6.45	−4.97	−3.52	2.13	0.45
L775	2.0	7.80	−5.24	−3.79	3.08	
	3.0	7.82	−5.21	−4.00	3.06	1.54
			4S662/L Blends			
L46	1.0	4.07	−3.40	−2.74	1.00	

[a] The plasticizer was 40 vol % DBP except for L775/DOP: T_r = 54 °C for all the L/DBP systems, and 71 °C for L775/DOP.[6]

In Figures 5–7, we see that the power law indexes of the terminal relaxation times, $J_{2,bB}\eta_{2,bB}$, to M_1 were determined to be 3.15 and 2.96 from least-squares fitting to the $J_{2,bB}\eta_{2,bB}$ data points (shown by the open symbols), respectively, for the 4S410/L and L2810/L blends with M_1 in the limited range of $M_2 \gg 172 \times 10^3 \geq M_1 > M_c$. (Note that M_2 is 1.64×10^6 for 4S410, and 2.81×10^6 for L2810.)

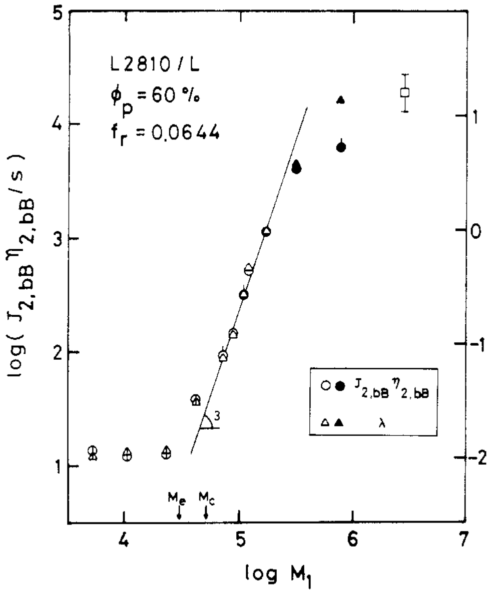

Figure 7. M_1 dependences of the weight average relaxation time $J_{2,bB}\eta_{2,bB}$ of the 2-chain in dilute L2810/L blends. The circles with pips indicate the data obtained in this study, and those without pips, our previous data.[6] The square indicates the extrapolated value for the L2810 system with $\phi_p = \phi_2$ = 60 vol % from the data for the L72 and L775 systems. For the triangles, see Figure 5 (and also the text).

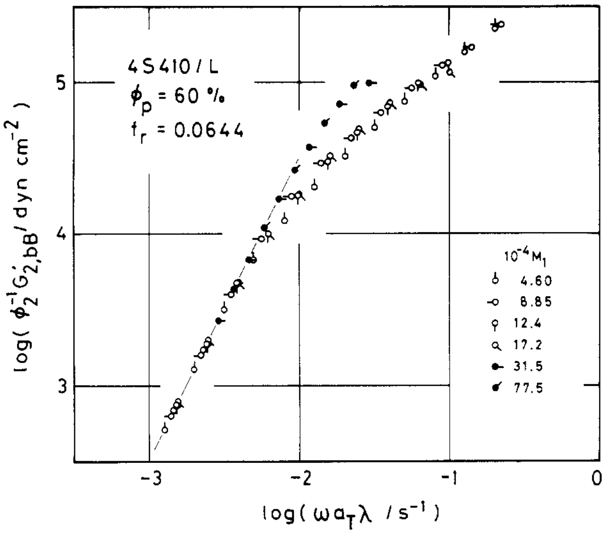

Figure 8. Test of the universality of the terminal relaxation modes in the dilute 4S410/L blends (see Discussion): comparison of the $G'_{2,bB}/\phi_2$ curves for the dilute 4S410/L blends with $M_1 > M_e$. For the blends with L46, L89, and L124, ϕ_2 = 1 vol %; for those with L172 and L315, ϕ_2 = 2 vol %; for the 4S410/L775 blend with ϕ_2 = 3 vol %. The original $\phi_2^{-1}G'_{2,bB}$ curve of each blend was shifted by an amount λ along the log ω axis so that the low-frequency end of the slope 2 was superposed to the one for the 4S410/L172 blend.

However, if we attempt a least-squares fitting of all the data points (including those shown by the solid symbols), we obtain for 4S410/L blends the index of 2.0 in those with $26.3 \leq 10^{-3}M_1 \leq 775$ and of 2.1 with $46.0 \leq 10^{-3}M_1 \leq 315$, and for L2810/L blends the index of 1.9 in those with $23.4 \leq 10^{-3}M_1 \leq 775$ and of 2.4 in those with $41.5 \leq 10^{-3}M_1 \leq 315$ (Figures 5 and 7). Obviously, if we pick up all the data points in the range of M_1 covered here, they cannot be represented by any power law relation.

On the other hand, the power law index of $J_{2,bB}\eta_{2,bB}$ to M_2 is 2.0 for the dilute 4S/L46 blends (cf. Figure 6) and also for dilute L/L blends with $M_c < M_1 \ll M_2$ (although the data are not shown here).[36]

Table IV
Zero-Shear Viscosity η_{bB}/P, Steady-State Compliance J_{bB}/(dyn^{-1} cm^2) of L2810/L Blends, and Compliance $J_{2,bB}$, Weight Average Relaxation Time $J_{2,bB}\eta_{2,bB}$/s, and Shift Factor λ of the L2810 Chain in the Blends with ϕ_P = 60 vol % and ϕ_2 = 1.0 vol % at T_r of an Isofree Volume Fraction State of f_r = 0.0644[a]

matrix[b]	log η_{bB}	log J_{bB}	log $J_{2,bB}$	log ($J_{2,bB}\eta_{2,bB}$)	log λ
L5	3.44	-2.38	-2.22	1.14	-1.98
L11	3.56	-2.58	-2.34	1.10	-1.94
L23	3.65	-2.76	-2.30	1.12	-1.93
L42	4.10	-2.76	-2.26	1.59	-1.51
L72	4.52	-2.90	-2.20	1.97	-1.12
L89	4.77	-2.92	-2.20	2.21	-0.87
L110	5.06	-2.94	-2.16	2.51	-0.56
L124	5.30	-2.92	-2.34	2.67	-0.38
L172	5.71	-3.04	-2.24	3.07	0
L315	6.51	-3.50	-2.30	3.61	0.57
L775	7.81	-4.82	-3.11	3.79	1.14

[a] Reproduced from ref 6. [b] The plasticizer was 40 vol % DBP except for L775/DOP: T_r = 44 °C for L5/DBP matrix; 49 °C for L11/DBP matrix; 54 °C for all other L/DBP systems; and 71 °C for L775/DOP.[6]

Table V
Zero-Shear Viscosity η_m and Steady-State Compliance J_m of Monodisperse 4S410 and L Samples with ϕ_P = 60 vol % at T_r[a] for an Isofree Volume Fraction State of f_r = 0.0644[b]

code	log (η_m/P)	log (J_m/(dyn^{-1} cm^2))
4S410[c]	8.96	-4.67
L5	2.68	-7.12
L11	2.96	-6.88
L23	3.27	-6.34
L26	3.33	-6.42
L42	3.75	-6.00
L46	3.80	-5.96
L72	4.27	-5.83
L89	4.53	-5.59
L110	4.84	-5.62
L124	5.00	-5.47
L172	5.50	-5.50
L315	6.39	-5.37
L775[c]	7.76	-5.36
L2810[d]	9.66	-5.40

[a] Reproduced from ref 6. [b] See the footnote of Table IV. [c] The plasticizer was 40 vol % DOP at T_r = 71 °C. [d] Extrapolated from the values of seven samples from L72 to L775.

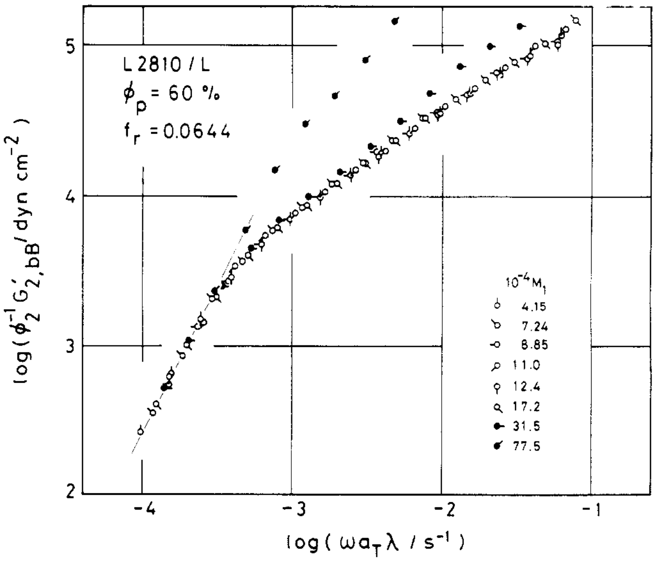

Figure 9. Test of the universality of the terminal relaxation modes in the dilute L2810/L blends (see Discussion): comparison of the $G'_{2,bB}/\phi_2$ curves for the dilute L2810/L blends with $M_1 > M_e$ and ϕ_2 = 1 vol %.

Discussion

Molecular Weight Dependences of Relaxation Times and Compliances. From Figures 5–7 we see that the relaxation times, $J_{2,\mathrm{bB}}\eta_{2,\mathrm{bB}}$, of the 2-chain in the dilute 4S410/L and L2810/L blends studied here may be cast into the power law form

$$J_{2,\mathrm{bB}}\eta_{2,\mathrm{bB}} \propto \phi_2{}^0 M_1{}^3 M_2{}^2 \tag{5}$$

as long as we consider the data obtained in the limited range of the molecular weights. The power law type $M_2{}^2$ dependence of the relaxation time is obeyed rather well for the entire range of M_2 examined, but the $M_1{}^3$ dependence is applicable only in the limited range of M_1 such that $M_c < M_1$ ($\leq 17.2 \times 10^4$ for these particular cases) $\ll M_2$.

The $M_1{}^3$ power law given in eq 5 is in agreement with the prediction of the tube model based on the tube renewal mechanism[26-28] for the relaxation of the test (2-) chain due to constraint release by diffusion of surrounding matrix (1-) chains. This result is consistent with an $M_1{}^{-3}$ dependence of the diffusion constant obtained from tracer diffusion experiment on linear polystyrenes.[12] On the other hand, the power law of $M_2{}^2$ in eq 5 is in agreement with the Rouse–Ham theory[24,25] for an isolated 2-chain, as will be discussed in the next section.

In this connection, we should comment on the results reported by Montfort and co-workers[8] for binary blends of linear PS and those of Roovers[11] for blends of linear and star polybutadienes (PB). Montfort and co-workers[8] determined a power law for the average relaxation time from Cole–Cole plots of the complex viscosity as $\bar{\tau} \propto M_1{}^{2.3}M_2{}^{1.9}$. On the other hand, Roovers[11] determined the longest relaxation time τ_1 defined as $\tau_1 = \omega^{-1}$ at $J'(\omega) = 0.9J_e{}^0$ from dynamic compliance data on dilute blends. He reported the relation $\tau_1 \propto M_1{}^{2.6}M_2{}^{2.2}$. Their results of the M_2 dependence of the relaxation times are in good agreement with our index of 2 to M_2 of $J_{2,\mathrm{bB}}\eta_{2,\mathrm{bB}}$. However, their indexes to M_1 are smaller compared with our value of 3.

Here, we should emphasize that for these power law indexes to be meaningful, the distribution of terminal relaxation modes of the 2-chain in the different blends must be the same. In other words, the terminal relaxation modes must be dominated by a common mechanism (or a common set of mechanisms). Here, we call this feature the *universality* of the terminal relaxation modes. For this is to be the case, the shape of the relaxation spectra, $H_{2,\mathrm{bB}}$, of the 2-chain of M_2 in the dilute blends should be independent of M_1, and thus superposable, at least, in their terminal regions by shifting alone the log τ axis. Thus, the storage moduli, $G'_{2,\mathrm{bB}}$, of the 2-chain should be superposable in their low-frequency regions by shifting along the log ω axis, because the $G'_{2,\mathrm{bB}}$ are far less sensitive to the fast modes of $H_{2,\mathrm{bB}}$ at short times τ (than the loss moduli, $G''_{2,\mathrm{bB}}$, are). The superposability of the low-frequency ends of $G'_{2,\mathrm{bB}}$ could be violated if the matrix components of different blends with a common 2-chain component have different M_1, and different relaxation mechanisms are involved in their terminal modes. Nevertheless, if we force $J_{2,\mathrm{bB}}\eta_{2,\mathrm{bB}}$ data for such blends having the terminal modes varying with M_1 to cast into a power law form, we should obtain only an artificial power law index.

A straightforward and reliable method of testing the data from this point of view is to see whether double logarithmic plots of the $G'_{2,\mathrm{bB}}$ versus ω of the 2-chain in dilute blends with different M_1 can be superposed, at least in the low-frequency range, by shifting the curves along the log ω axis. To see whether the above criterion is satisfied or not, we compared the shape of the $\phi_2{}^{-1}G'_{2,\mathrm{bB}}$ curves defined by eq 3a for the dilute 4S410/L blends with varying M_1 as follows. Each curve was shifted by an amount λ along the log ω axis so that the low-frequency ends of all the curves (with the slope 2) were superposed to the curve for the 4S410/L172 blend. Figure 8 shows the results of such a test in the form of $\phi_2{}^{-1}G'_{2,\mathrm{bB}}$ versus $\omega a_T\lambda$ plots, and Figure 9 shows similar plots for the dilute L2810/L blends with $M_1 > M_e$.

In Figure 8, we see that the portions of the low-to-intermediate frequency range of the $G'_{2,\mathrm{bB}}$ curves (open circles) for the 4S410/L blends with $M_1 < 172 \times 10^3$ are nicely superposed to the curve of the 4S410/L172 blend, but those (closed circles) of the blends with $M_1 \geq 315 \times 10^3$ start deviating from the composite curve. The shape of the terminal zones of the similar curves for the L2810/L blends with M_1 even below M_e obtained in our previous study[6] was the same with the composite curve shown in Figure 9.

The values of the shift parameter λ used to obtain the composite curves in Figures 8 and 9 were also plotted (by open or closed triangles) in Figures 5 and 7, respectively, and also summarized in Tables III and IV. We see that the M_1 dependences of λ for the blends with $M_1 \leq 172 \times 10^3$ nicely conform to that of $J_{2,\mathrm{bB}}\eta_{2,\mathrm{bB}}$ of the 2-chain in these dilute blends.

Thus, from these critical tests shown in Figures 8 and 9, we confirmed that the power law index to M_1 is very close to 3 (but not to 2.0–2.5) for the data points of the dilute blends in the entangled and universal region ($M_c < M_1 \ll M_2$). Although the universality of the terminal relaxation modes still remains valid for the dilute blends of the 2-chain with the matrix chain of $M_1 \lesssim M_c$ (or M_e), the average relaxation times become insensitive to the variation in M_1, as seen in Figures 5 and 7, by an obvious reason that the matrix 1-chains are no longer effectively entangling with the 2-chain. We should not include the data points of such nonentangling blends for estimating the power law index to M_1.

The values of 2–2.5 for the power law index of the relaxation time to M_1 reported by Montfort[8] and by Roovers[11] are smaller than our index of 3. For this discrepancy between their and our results, we first notice that their relaxation times are not well-defined ones and cannot be represented by any simple functions of the test-chain relaxation spectra, $H_{2,\mathrm{bB}}$, as opposed to ours, which were defined by eq 4d as the weight average values. In addition to test the distribution of the terminal relaxation modes, Roovers[11] employed the subscribed angle tan β of the Cole–Cole plots and pointed out that tan β increases as the size of the test chain, M_2, increases; it appears to be independent of ϕ_2, but its dependence on the matrix molecular weight, M_1, is unclear.[11] Thus, the most crucial point in testing the validity of the power law index of $J_{2,\mathrm{bB}}\eta_{2,\mathrm{bB}}$ to M_1 remains ambiguous.

Since they did not fully establish the universality of the terminal relaxation modes in the manner we suggested above, we cannot judge whether their power law indexes are representing the true asymptotic values or not. The discrepancy between their and our power law indexes for M_1 may be explained, at least partly, from this point of view.[37]

Compliance of the Star Chains. The Rouse–Ham theory[24,25] predicts the compliance $J_{2,\mathrm{bB}}$ of an isolated 2-chain as

$$J_{2,\mathrm{bB}} = 2g_2M_2/(5\rho\phi_2RT); \quad g_2 = (15f - 14)/(3f - 2)^2 \tag{6}$$

where f is the number of arms of the 2-chain (thus, $f = 4$ for 4S chains and 2 for L chains), ρ is the bulk density of the polymer, and RT has the usual meaning. Strictly

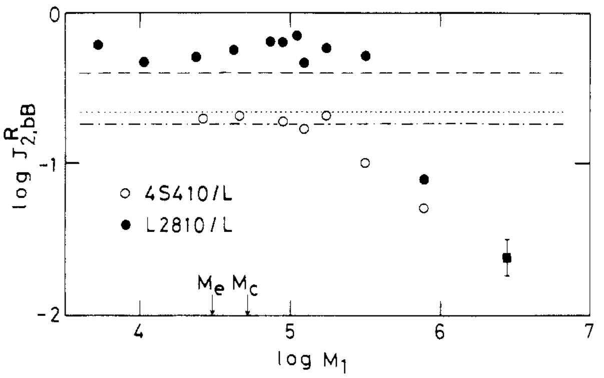

Figure 10. Plots of the reduced compliances $J^R_{2,bB}$ of the 2-chain versus M_1 for dilute 4S410/L and L2810/L blends. The solid square and the dotted line indicate the values for the monodisperse L2810 and 4S410 systems with $\phi_p = \phi_2 = 60$ vol %, respectively. The broken and dash–dot lines indicate the theoretical values of the Rouse–Ham theory (eq 6 and 7) for the L and 4S chains, respectively.

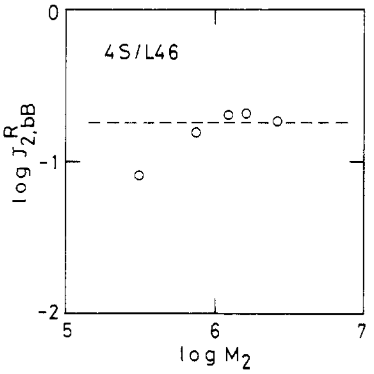

Figure 11. Plots of the reduced compliance $J^R_{2,bB}$ of the star 2-chain versus M_2 for the dilute 4S/L46 blends. The broken line indicates the prediction of the Rouse–Ham theory (eq 6 and 7).

speaking, $\rho\phi_2$ in eq 6 must be the weight concentration c (g/cm^3) of the 2-chain in the blend or in solution. However, we neglected this small density difference and assumed c to be equal to $\rho\phi_2$.

Thus, the compliance, $J_{2,bB}$, of the isolated 2-chain may be more conveniently represented by the reduced compliance, $J^R_{2,bB}$, defined as

$$J^R_{2,bB} = \rho\phi_2 RT J_{2,bB}/M_2 = 2g_2/5 \qquad (7)$$

The third term is the prediction of the Rouse–Ham theory.[24,25]

Figure 10 shows the M_1 dependence of $J^R_{2,bB}$ of the dilute 4S410/L and L2810/L blends. (The dotted line in the figure shows the level of the reduced compliance of the monodisperse 4S410 system, while the filled square shows the value of the monodisperse L2810 system, both with $\phi_2 = \phi_p = 60$ vol %.) We notice that the $J^R_{2,bB}$ of these blends are nearly independent of M_1 as long as M_1 ($\leq 172 \times 10^3$) $\ll M_2$ but begin to deviate downward as M_1 is increased close to M_2.

On the other hand, Figure 11 shows the M_2 dependence of $J^R_{2,bB}$. Thus, the $J_{2,bB}$ data can be cast into the form

$$J_{2,bB} \propto \phi_2^{-1} M_2 M_1^0 \qquad (8)$$

again, as long as $M_1 \ll M_2$.

We can also check the universality of the terminal relaxation modes in these blends by comparing the reduced compliances, $J^R_{2,bB}$, shown in Figures 10 and 11, since these quantities are very sensitive to the distribution of the terminal relaxation modes. Obviously, all the blends with M_1 in the limited region of $M_1 \ll M_2$, where the universality of the terminal modes is valid, satisfy the power law of eq 8.

In Figures 4a, 10, and 11, the compliances predicted by eq 6 and 7 are shown by the broken lines (and/or dash–dot line). Note that $J^R_{2,bB}$ for 4S410 is significantly smaller than the theoretical value (=0.4 by eq 6 with $g_2 = 2$) for the linear chain. The compliances of both 4S and L chains in the dilute blends are close to the prediction of the Rouse–Ham theory as long as $M_1 \ll M_2$.[36]

Relaxation Mechanisms of the Test Chain in Dilute Blends. Now returning to the question of the M_2 dependence of $J_{2,bB}\eta_{2,bB}$ of an isolated chain, we notice the following. The Rouse–Ham theory predicts that the relation between the relaxation times of an isolated f-arm star chain of M_2 is

$$(J_{2,bB}\eta_{2,bB})_{\text{star}} = g_1 g_2 (J_{2,bB}\eta_{2,bB})_{\text{linear}} \propto g_1 g_2 M_2^2 \qquad (9a)$$

$$g_1 = (3f-2)/f^2 \qquad (9b)$$

Although the original Rouse–Ham theory[24,25] is derived for an isolated and nonentangling chain in dilute solution, we may apply the theory to the test 2-chain in dilute blends, if the monomeric friction coefficient ζ_0 in the original theory can be replaced by an effective friction coefficient representing the retarded motion of the 2-chain due to entanglement with the matrix (1-) chains. This approximation should be valid if 1–2 entanglement affects only the local friction or the local jump frequency of the segments of the 2-chain. Then, introducing the data for the dilute L/L blends obtained in the universal and entangled region shown in Figure 7 into eq 9a, we should be able to deduce the relaxation times of the f-arm star chain in the dilute blend. The result was indicated by the broken line in Figure 5, in which we see that the observed $(J_{2,bB}\eta_{2,bB})_{\text{star}}$ values in the region of $M_c < M_1 \ll M_2$ are about half of the Rouse–Ham values estimated by eq 9a as mentioned above.

Thus, we may say as a crude approximation that the 2-chain in the dilute blend relaxes by the Rouse–Ham-like mechanism retarded to an extent of the time scale of constraint release by the tube renewal mechanism. However, strictly speaking, the small but significant discrepancy between the observed and theoretical values of the relaxation times suggests that the dynamics of the 2-chain appears to be not completely the same as the dynamics predicted by the Rouse–Ham theory. This is presumably because 1–2 entanglements are still effective at short times. We reached the similar conclusion by comparing the diffusion and viscoelastic data of dilute L/L blends of narrow-MWD polystyrenes.[36]

As repeatedly emphasized in the previous sections, the M_1^3 dependence of the average relaxation times of an isolated 2-chain is valid only in the limited range of the molecular weights of the dilute blends involved. Aside from the crucial problem on the exact value of the power law index for the tube renewal mechanism, we may say that any power laws of a single index may not be valid for the entire range of M_1 and M_2 of dilute blends. The reasons are as follows.

In the dilute blends with small M_1 ($<M_e$), the 2-chain relaxes by the intrinsic Rouse–Ham modes, and the relaxation times are independent of M_1.[5,6] The horizontal dash–dot line in Figure 5 shows this intrinsic relaxation time for 4S410 estimated by applying eq 9 to the data in Figure 7 for the linear 2-chain in the dilute blends with $M_1 < M_e$. The average relaxation time, $(J_{2,bB}\eta_{2,bB})_{\text{star}}$, of an isolated star as well as linear chain approaches this intrinsic Rouse–Ham value as M_1 decreases to M_e. This is practically the lower bound of $J_{2,bB}\eta_{2,bB}$ of the 2-chain.

On the other hand, for the blends with $M_1 > M_c$, as M_1 is increased close to or even to exceed M_2, the dominant modes can no longer be the retarded Rouse–Ham-like modes but can be, in terms of the tube theory, *reptation* for linear chains and *path breathing* for star chains.[28] The relaxation times are strongly dependent on M_2 but nearly independent of M_1.[40] Thus, the dotted line in Figure 5 shows the level of $J_{2,\mathrm{bB}}\eta_{2,\mathrm{bB}}$ for the monodisperse 4S410 system, and the open square in Figure 7 indicates the value of $J_{2,\mathrm{bB}}\eta_{2,\mathrm{bB}}$ for the monodisperse L2810 system, both with $\phi_2 = \phi_\mathrm{p} = 60$ vol %.

For the dilute blends with $M_2 \gg M_1 > M_c$, the relaxation of the test chain may proceed via the following steps.[3-6,36] First, the surrounding matrix (1-) chains diffuse away and release the constraint imposing on the 2-chain. In the framework of the tube model, this process corresponds to tube renewal.[27,28,38] Random local jumps of the segments of the 2-chain take place, simultaneously activating the Rouse–Ham modes to relax the chain itself.

As M_1 and M_2 become closer, competition between the tube renewal process and other potentially active modes such as reptation (for a linear chain) or path breathing (for a star chain) takes place. The retarded Rouse–Ham-like modes are no longer the overwhelming modes. The decrease in $J_{2,\mathrm{bB}}$ and $J^\mathrm{R}_{2,\mathrm{bB}}$ (Figures 4a, 10, and 11) and changes in $\phi_2^{-1}G'_{2,\mathrm{bB}}$ (Figures 8 and 9) reflect such a situation. Thus, the power law relation of $J_{2,\mathrm{bB}}\eta_{2,\mathrm{bB}} \propto M_1^3$ should be observed only for the blends with $M_2 \gg M_1 > M_c$, in which the retarded Rouse–Ham-like modes proceed *much* faster than the reptation or path-breathing relaxation modes for the monodisperse 2-chain.

It is interesting to note that the span of M_1, in which the M_1^3 power law is valid, is nearly the same for the dilute 4S410/L and L2810/L blends (cf. Figures 5 and 7), although M_2 of the former is considerably smaller than that of the latter. This result suggests that the essential factor governing the above-mentioned competition is not the M_2/M_1 ratio but the ratio of the longest relaxation times of the two competing processes.[41] In this connection, we see in Figures 5 and 7 that the weight average relaxation times are nearly the same for the bulk 4S410 and L2810 systems. The time constant of the path-breathing modes for a star chain increases exponentially with M_2 (or M_a) and exceeds at certain M_2 the time constant of the reptation modes for the corresponding linear chain. Thus, even in the dilute blends of the star (2-) chain in the matrix with fairly large M_1 (relative to M_2), the Rouse–Ham-like modes retarded by the tube renewal mechanism still overwhelm the path-breathing modes, which are dominant in star (2-) chain in the monodisperse bulk state. This expectation is consistent with the results demonstrated in Figure 5 and 7.

Acknowledgment. We acknowledge with thanks financial support from the Ministry of Education, Science, and Culture (Mombusho), Japan, under Grant 6047107.

Registry No. Polystyrene, 9003-53-6.

References and Notes

(1) Ferry, J. D. *Viscoelastic Properties of Polymers*, 3rd ed.; Wiley: New York, 1980.
(2) Graessley, W. W. *Adv. Polym. Sci.* **1974**, *16*, 1.
(3) Watanabe, H.; Kotaka, T. *Macromolecules* **1984**, *17*, 2316.
(4) Watanabe, H.; Sakamoto, T.; Kotaka, T. *Macromolecules* **1985**, *18*, 1008.
(5) Watanabe, H.; Sakamoto, T.; Kotaka, T. *Macromolecules* **1985**, *18*, 1436.
(6) Watanabe, H.; Kotaka, T. *Macromolecules* **1986**, *19*, 2520.
(7) Watanabe, H.; Kotaka, T. *Macromolecules* **1987**, *20*, 535.
(8) Montfort, J.-P.; Marin, G.; Monge, P. *Macromolecules* **1984**, *17*, 1551.
(9) Montfort, J.-P.; Marin, G.; Monge, P. *Macromolecules* **1986**, *19*, 1979.
(10) Struglinski, M. J.; Graessley, W. W. *Macromolecules* **1985**, *18*, 2630.
(11) Roovers, J. *Macromolecules* **1987**, *20*, 148.
(12) Green, P. F.; Mills, P. J.; Palmstrøm, C. J.; Mayer, J. W.; Kramer, E. J. *Phys. Rev. Lett.* **1984**, *53*, 2145.
(13) Green, P. F.; Kramer, E. J. *Macromolecules* **1986**, *19*, 1108.
(14) Antonietti, M.; Coutandin, J.; Grütter, R.; Silescu, Hh. *Macromolecules* **1984**, *17*, 798.
(15) Antonietti, M.; Coutandin, J.; Sillescu, H. *Macromolecules* **1986**, *19*, 793.
(16) Masuda, T.; Ohta, Y.; Onogi, S. *Macromolecules* **1971**, *4*, 763.
(17) Graessley, W. W.; Masuda, T.; Roovers, J.; Hadjichristidis, N. *Macromolecules* **1976**, *9*, 127.
(18) Graessley, W. W.; Roovers, J. *Macromolecules* **1979**, *12*, 959.
(19) Raju, V. R.; Menezes, E. V.; Marin, G.; Graessley, W. W.; Fetters, L. J. *Macromolecules* **1981**, *14*, 1668.
(20) Kajiura, H.; Ushiyama, Y.; Fujita, T.; Nagasawa, M. *Macromolecules* **1978**, *11*, 894.
(21) Roovers, J. *Macromolecules* **1984**, *17*, 1196.
(22) Roovers, J. *Macromolecules* **1985**, *18*, 1359.
(23) McKenna, G. B. *Faraday Symp. Chem. Soc.* **1983**, *18*, 210. Also: McKenna, G. B.; Hadziioannou, G.; Lutz, P.; Hild, G.; Strazielle, C.; Straupe, C.; Rempp, P.; Kovacs, A. J. *Macromolecules* **1987**, *20*, 498.
(24) Rouse, P. E. *J. Chem. Phys.* **1953**, *21*, 1272.
(25) Ham, J. S. *J. Chem. Phys.* **1957**, *26*, 625.
(26) Doi, M.; Edwards, S. F. *The Theory of Polymer Dynamics*; Clarendon Press: Oxford, 1986.
(27) Klein, J. *Macromolecules* **1978**, *11*, 852.
(28) Graessley, W. W. *Adv. Polym. Sci.* **1982**, *47*, 67.
(29) Gervasi, J. A.; Gosnell, A. B. *J. Polym. Sci. Polym. Chem. Ed.* **1966**, *4*, 1391.
(30) Hadjichristidis, N.; Roovers, J. *J. Polym. Sci., Polym. Phys. Ed.* **1974**, *12*, 2521.
(31) Morton, M.; Fetters, L. J. *Rubber Chem. Technol.* **1975**, *48*, 359.
(32) Fujimoto, T.; Nagasawa, M. *Advanced Techniques for Polymer Synthesis*; Kagaku-dojin: Kyoto, 1972.
(33) Arai, K.; Kotaka, T.; Kitano, Y.; Yoshimura, K. *Macromolecules* **1980**, *13*, 1670. Kudose, I.; Kotaka, T. *Ibid.* **1984**, *17*, 2325.
(34) Roovers, J.; Bywater, S. *Macromolecules* **1972**, *5*, 384.
(35) The critical volume fraction ϕ_2 corresponding to onset of entanglements among the star 2-chains (4S410) may be estimated in two different ways as[11,17] $(\phi_2)_c = M_c°/(g_1M_2) \simeq 3.0$ vol %; $(\phi_2)_c' = M_e°/M_a \simeq 4.4$ vol % with the arm molecular weight M_a of the star sample, the characteristic molecular weight $M_c°$ ($\simeq 31 \times 10^3$), and the entanglement spacing $M_e°$ ($\simeq 18 \times 10^3$) for bulk PS.[1] The factor g_1 ($\simeq 0.625$ for 4-arm star chain) is defined in eq 9b. The critical values of 3–5 vol % found for the 4S410 sample fall within the range predicted as above. A similar result was found also for blends of linear chain PS.[3]
(36) Watanabe, H.; Kotaka, T. *Macromolecules* **1987**, *20*, 530.
(37) On the basis of the tube renewal concept, Montfort and coworkers[8] interpreted their small power law index of 2.3 as due to the interdependence of the effective constraints for the 2-chain. Klein[38] suggested that the index should be 2.5 for such cases. However, de Gennes[39] discussed effective constraints becoming interdependent in the blends with very large M_1. As shown in this and previous papers,[5] the power law type M_1^3 dependence of the relaxation times is observable only in the limited range $M_c < M_1 \ll M_2$. This condition cannot be satisfied easily for the blends with large M_1 ($\gg M_c$) because of the limitation from M_2. Thus, for blends involving PS, which has the relatively large M_c^0, the idea of the interdependent constraint appears to be inadequate to explain the small power law index of $M_1^{2.3}$.
(38) Klein, J. *Macromolecules* **1986**, *19*, 105.
(39) de Gennes, P.-G. *Macromolecules* **1986**, *19*, 1245.
(40) Obviously, the behavior of the L/L blends approaches that of the monodisperse bulk system as M_1 approaches M_2.[36] However, even if $M_1 = M_2$, the star/linear chain blends obviously differ from the monodisperse star chain system.
(41) For the L/L blends, obviously, the M_2/M_1 ratio or the factor $M_2M_e^2M_1^{-3}$ proposed by Struglinski and Graessley[10] and also by Green and co-workers[12] are governing the competition of the possible modes.